JPn Neuroscience
The Journal of Physiology

Modulation of spike clustering by NMDA receptors and neurotensin in rat supraoptic nucleus neurons

Ariane Gagnon, Michael Walsh, Tika Okuda, Katrina Y. Choe, Cristian Zaelzer and Charles W. Bourque

Centre for Research in Neuroscience, Research Institute of the McGill University Health Centre, Montreal QC, Canada H3G 1A4

Key points

- Magnocellular neurosecretory cells (MNCs) of the rat supraoptic nucleus adopt bursting activity patterns under conditions demanding maximum peptide release from their nerve endings in the neurohypophysis.
- Exogenous activation of NMDA receptors (NMDARs) induces spike clustering in MNCs through a mechanism that requires apamin-sensitive small conductance calcium-activated K^+ (SK) channels).
- Here we show that NMDAR- and SK channel-dependent spike clustering can be induced in MNCs by release of endogenous glutamate from afferent axon terminals.
- This form of bursting activity can be modulated by subtle changes in membrane voltage, or by partial inhibition of SK channels.

Abstract Magnocellular neurosecretory cells (MNCs) in the rat supraoptic nucleus display clustered firing during hyperosmolality or dehydration. This response is beneficial because this type of activity potentiates vasopressin secretion from axon terminals in the neurohypophysis and thus promotes homoeostatic water reabsorption from the kidney. However, the mechanisms which lead to the generation of clustering activity in MNCs remain unknown. Previous work has shown that clustered firing can be induced in these neurons through the pharmacological activation of NMDA receptors (NMDARs) and that silent pauses observed during this activity are mediated by apamin-sensitive calcium activated potassium (SK) channels. However, it remains unknown if clustered firing can be induced *in situ* by endogenous glutamate release from axon terminals. Here we show that electrical stimulation of glutamatergic osmosensory afferents in the organum vasculosum lamina terminalis (OVLT) can promote clustering in MNCs via NMDARs and apamin-sensitive channels. We also show that the rate of spike clustering induced by NMDA varies as a bell-shaped function of voltage, and that partial inhibition of SK channels can increase cluster duration and reduce the rate of clustering. Finally, we show that MNCs express neurotensin type 2 receptors, and that activation of these receptors can simultaneously depolarize MNCs and suppress clustered firing induced by bath application of NMDA or by repetitive stimulation of glutamate afferents. These studies reveal that spike clustering can be induced in MNCs by glutamate release from afferent nerve terminals and that that this type of activity can be fine-tuned by neuromodulators such as neurotensin.

(Received 5 April 2014; accepted after revision 9 July 2014; first published online 25 July 2014)
Corresponding author C. Bourque: Division of Neurology L7-216, Montreal General Hospital, 1650 Cedar Ave, Montreal QC, Canada H3G1A4. Email: charles.bourque@mcgill.ca

Abbreviations APV, D,L-amino-phosphono-valerate; CPM, clusters per minute; MNC, magnocellular neurosecretory cell; NMDAR, *N*-methyl-D-aspartate receptor; NT, neurotensin; NTS, neurotensin receptor; OVLT, organum vasculosum lamina terminalis; SK, small conductance potassium (channel); SON, supraoptic nucleus.

DOI: 10.1113/jphysiol.2014.275602

Introduction

Bursting electrical activity is involved in many aspects of brain function, but the mechanisms by which it can be induced or modulated are poorly understood (McGinty & Szymusiak, 1988; Krahe & Gabbiani, 2004). Phasic activity and clustered firing are two distinct forms of rhythmic bursting that emerge from rat magnocellular neurosecretory cells (MNCs) during dehydration and hyperosmolality both *in vivo* (Poulain *et al.* 1988) and *in vitro* (Bourque & Renaud, 1984). Phasic activity is characterized by alternating periods of action potential (spike) discharge and silent intervals lasting 20–60 s each, whereas clustered firing features briefer bursts of spikes (~0.2–5 s) separated by pauses of comparable duration (Poulain *et al.* 1988; Hu & Bourque, 1992). The emergence of bursting patterns under conditions requiring water conservation is physiologically important because phasic activity and clustered firing have both been shown to facilitate the secretion of antidiuretic hormone (vasopressin) from the axon terminals of MNCs in the neurohypophysis (Dutton & Dyball, 1979; Cazalis *et al.* 1985). Although much is known about the processes which mediate phasic activity (Brown & Bourque, 2006), little is known of the mechanisms that induce or modulate clustering activity.

Previous work *in vitro* has shown that pharmacological activation of *N*-methyl-D-aspartate (NMDA) receptors (NMDARs) can induce clustering activity in MNCs, and that pauses observed during NMDA-induced clustered firing are eliminated by apamin (Hu & Bourque, 1992), a selective inhibitor of small conductance calcium-dependent K^+ channels (i.e. SK channels) (Faber, 2009). Given the strong voltage dependency of NMDA receptors (Monyer *et al.* 1994), is it likely that clustered firing mediated by such a mechanism could be modulated either through a regulation of SK channels, or by changes in the membrane potential of the target cell. However, it remains unknown if NMDAR- and SK channel-dependent clustered firing can be induced by endogenous release of glutamate *in situ*.

Osmosensitive neurons in the organum vasculosum of lamina terminalis (OVLT) are excited under hyperosmotic conditions (Ciura & Bourque, 2006; Ciura *et al.* 2011) and these neurons send glutamatergic afferents onto MNCs in the supraoptic nucleus (SON; Richard & Bourque, 1995; Armstrong *et al.* 1996). In this study we therefore examined if activation of OVLT neurons can promote the emergence of NMDAR-dependent clustered firing in MNCs, and if this type of activity can be modulated by neurotensin (NT), a neuropeptide known to affect the membrane potential of MNCs (Kirkpatrick & Bourque, 1995; Chakfe & Bourque, 2000).

Methods

Adult male Long Evans rats (80–160 g) were killed by decapitation in accordance with a protocol approved by McGill University's Facility Animal Care Committee (Protocol No. 1190) and brain brains were rapidly extracted for preparation of hypothalamic slices or explants, or to harvest blocks of SON tissue used for PCR analysis.

Whole-cell recordings in slices

Angled horizontal hypothalamic slices (400 μm thick) prepared as described previously (Trudel & Bourque, 2010) were perfused at 31–33°C (2 ml min^{-1}) with carbogenated (95% O_2, 5% CO_2) artificial cerebrospinal fluid (ACSF) comprising (in mM): 120 NaCl, 4 KCl, 1.46 $MgCl_2$, 26 $NaHCO_3$, 2 $CaCl_2$, 1.23 NaH_2PO_4, 10 D-glucose (all from Sigma-Aldrich Co., Oakville, Ontario, Canada). Whole-cell recordings were made using pipettes prepared with a P-87 puller (Sutter Instrument, Novato CA) and filled with a solution comprising (in mM): 110 $KMeSO_4$, 10 Hepes, 10 KCl, and 1 $MgCl_26H_2O$ (2–5 MΩ). Clusters were detected using a procedure modified from the Poisson surprise technique (Ko *et al.* 2012), where individual clusters were identified as groupings of ≥2 action potentials separated by interspike intervals lasting more than the pause criterion (PC), defined as the duration beyond which fewer than 1% of the interspike intervals are expected to occur as determined by fitting a single exponential to the falling phase of the interspike interval distribution measured in each cell (see Fig. 2*B*). Graphs showing the voltage dependency of clustering were generated by interpolating and aligning data obtained from different cells in 2.5 mV increments.

Extracellular recording in hypothalamic explants

Hypothalamic explants prepared as previously described (Choe *et al.* 2012) were superfused with carbogenated ACSF containing 1 mM $CaCl_2$ (32°C; 1 ml min^{-1}). Recording micropipettes prepared with a vertical puller (Narighige International USA, INC., East Meadow, NY) were filled with 1 M NaCl (10–20 MΩ) and advanced using an IVM micromanipulator (Scientifica, Uckfield, UK). Voltage recorded via an Axoclamp-2A (Molecular Devices Corp, Sunnyvale, CA, USA) was filtered (0.5−1.2 kHz) before capture using Clampex 10 software (Molecular Devices). Cells with a basal firing frequency ≥10 Hz or a basal rate of clustering ≥12 clusters per minute (CPM) were excluded from analysis. Because electrically evoked clustering was short lived, the number of interspike intervals detected during this period was insufficient to produce a histogram that could be adequately fitted with a single exponential function. Therefore individual

clusters recorded in explants were arbitrarily defined as a grouping of two or more action potentials preceded and followed by pauses greater than 400 ms, and where inter-spike intervals within the cluster were smaller than 400 ms (as previously described; Hu & Bourque, 1992).

Drugs

Stocks of apamin, NT and NT fragments (10^{-3} M; Sigma-Aldrich) dissolved in water (10^{-4} M), or SR46892 dissolved in DMSO (10^{-3} M; provided by Dr P. Sarret), were kept frozen and dissolved as needed into ACSF. NMDA and the NMDAR antagonist D,L-amino-phosphono-valeric acid (APV; both from Sigma) were freshly dissolved into ACSF.

Tissue and single-cell PCR

Blocks of SON tissue were placed in RNAlater (Life Technologies Inc., Burlington, ON, Canada) or processed as previously decribed to isolate MNCs (Sharif Naeini *et al.* 2006). Tissue RNA was purified and converted to cDNA using RiboPure and RETROscript kits (Life Technologies). For single cell analysis, MNCs were aspirated into a micropipette containing 1.5 μl Hepes buffer with RNAseIN (10 U μl^{-1}) and then expelled into a tube containing 0.5 μl DNAse I (1 U μl^{-1}) and 0.5 μl buffer (Fermentas), incubated at 37°C for 30 min, after which 1 μl 25 mM EDTA was added. Retrotranscription was performed with 1 μl 50 μM Random Hexamer primers, 0.25 μl RNAseIN (10 U μl^{-1}), 1 μl 0.1 M DTT, 1 μl 50 mM $MgCl_2$, 1 μl 10 mM (each) dNTPs mix (Qiagen), 2 μl First Strand Buffer and 0.25 μl SuperscriptIII (200 U μl^{-1}) (Life Technologies). The mix was incubated at 50°C for 2 h and the resulting cDNA was stored at −20°C. PCR detection of NT receptors 1 (NTS1) and 2 (NTS2) was performed using a nested approach with Phusion High Fidelity Polymerase (New England Biolabs, Whitby, ON, Canada). Primers targeting NTS1 were: external pair, forward (5′GGTAGCCGTGTGTGCGCTCC3′), reverse (5′AAAGGGCTGGGCATCGGGTTC3′), expected product 489 bp; internal pair, forward (5′ATCTGGAGGTCC GTAGCAGCCC3′), reverse (5′GTTGAGGTGCATGGTG GGTGCC3′), expected product 322 bp. For NTS2. the primers were: external pair, forward (5′GCTGTCACT GGTCTGGGTCGC3′), reverse (5′GTGCTGGAGGCTGC GGATCTG3′), expected product 418 bp; internal pair, forward (5′AGCACGAAGTGGAAAGCGCGG3′), reverse (5′CGTGATGAAGCCCAGGAGGCC3'), expected product 272 bp.

Statistics

All values are reported as means ± SEM Sigmaplot 12 (Systat Software Inc., Chicago, IL, USA) was used to perform statistical tests including: Student's *t* test, paired *t* test; one-way ANOVA, followed by the Holm–Sidak *post hoc* test; one-way repeated measures (RM) ANOVA, followed by the Holm–Sidak *post hoc* test. A value of $P < 0.05$ was considered statistically significant.

Results

To determine if NMDAR-dependent clustering can be induced by endogenous glutamate release, we examined the effects of electrically stimulating the OVLT during extracellular recordings of single unit spiking activity from MNCs in superfused explants of rat hypothalamus. As illustrated in Fig. 1*A*, repetitive electrical stimulation of the OVLT at 10 Hz for 60 s induced spike clusters that were not observed during the pre-stimulation period. In other cells, clustering could be observed during the baseline period, and in these cases the rate of clustering was reversibly enhanced by OVLT stimulation (not shown). The average rate of clustering measured during consecutive 30 s intervals returned exponentially to baseline following the end of the stimulus (Fig. 1*B*; $\tau = 49.6$ s; $n = 5$). While OVLT stimulation at 10 Hz for 10−30 s did not affect the rate of clustering observed during the first 20 s after the end of the train ($n = 8$; one-way repeated measures ANOVA with *post hoc* Holm–Sidak test; $P = 0.842$), stimulating the OVLT for 60 s caused a significant increase in clustering (Fig. 1*C*; from 4.6 ± 1.1 to 15.7 ± 4.0 CPM; $n = 13$; one-way RM ANOVA with *post hoc* Holm–Sidak test; $P = 0.003$).

To determine if NMDARs are involved in OVLT-mediated spike clustering, we examined the effects of blocking these receptors with APV (100 μM). In the presence of APV, stimulation of the OVLT for 60 s (10 Hz) no longer increased the rate of clustering (Fig. 1*D* and *E*; $n = 7$; one-way RM ANOVA with *post hoc* Holm–Sidak test; $P = 0.882$). We next examined if OVLT-mediated clustering required the activity of SK channels. As shown in Fig. 1*D* and *E*, bath application of the SK channel inhibitor apamin (100 nM) prevented the increase in the rate of clustering induced by OVLT stimulation ($n = 6$; one-way RM ANOVA with *post hoc* Holm–Sidak test; $P = 0.909$). Collectively, these results indicate that endogenous activity-dependent glutamate release can induce clustered firing in MNCs, through a mechanism that depends on NMDAR activation and SK channel activity.

To determine if changes in membrane potential can affect clustered firing, we examined the effects of current injection on NMDAR-induced clustering activity during whole-cell patch clamp recordings in hypothalamic slices. As illustrated in Fig. 2*A* and *B*, bath application of 50 μM NMDA caused a depolarization of the membrane potential and the emergence of sustained clustering activity that persisted throughout the application. Cells were then hyperpolarized until silenced and then a

staircase of incrementing current steps (+5 pA, 30 s each) was delivered until the cell was strongly depolarized. As illustrated in Fig. 2*C*, cells exposed to ACSF did not display clustering activity at any of the voltages examined, whereas cells exposed to NMDA displayed robust clustering activity. The relationship between the rate of clustering and voltage in NMDA-treated cells was bell shaped, with a maximum at −65 mV (Fig. 2*D*; ACSF $n = 10$, NMDA $n = 35$). Based on the shape of this curve, we expect that membrane depolarization from initial voltages ≤−65 mV would enhance clustering as long as voltage does exceed −65 mV, whereas depolarization from baseline voltages between −65 and −50 mV would reduce clustering activity. Indeed as illustrated in Fig. 2*E*, depolarizing current steps applied from −83 and −65 mV respectively induced or suppressed clustered firing. These results suggest that neurotransmitters capable of changing the membrane potential could regulate the rate of NMDAR-driven clustering activity in MNCs.

In agreement with previous work (Hu & Bourque, 1992), NMDAR-dependent clustering activity was fully inhibited by bath application of a saturating concentration of apamin to block SK channels (100 nM; Fig. 3*A*). To determine if a more partial inhibition of SK channels can modulate clustered firing we examined the effects of a submaximal dose of apamin. Using whole-cell recording we found that the after-hyperpolarization following a current-induced spike train was only partly (~25%) yet significantly reduced by 4 nM apamin (Fig. 3*B* and *C*; $n = 12$; paired *t* test; $P = 0.001$). We therefore examined the effects of 4 nM apamin on NMDA-evoked clustered firing using the staircase protocol described earlier. Apamin (4 nM) caused a significant decrease in the rate of NMDA-evoked clustering at voltages between −62.5 and

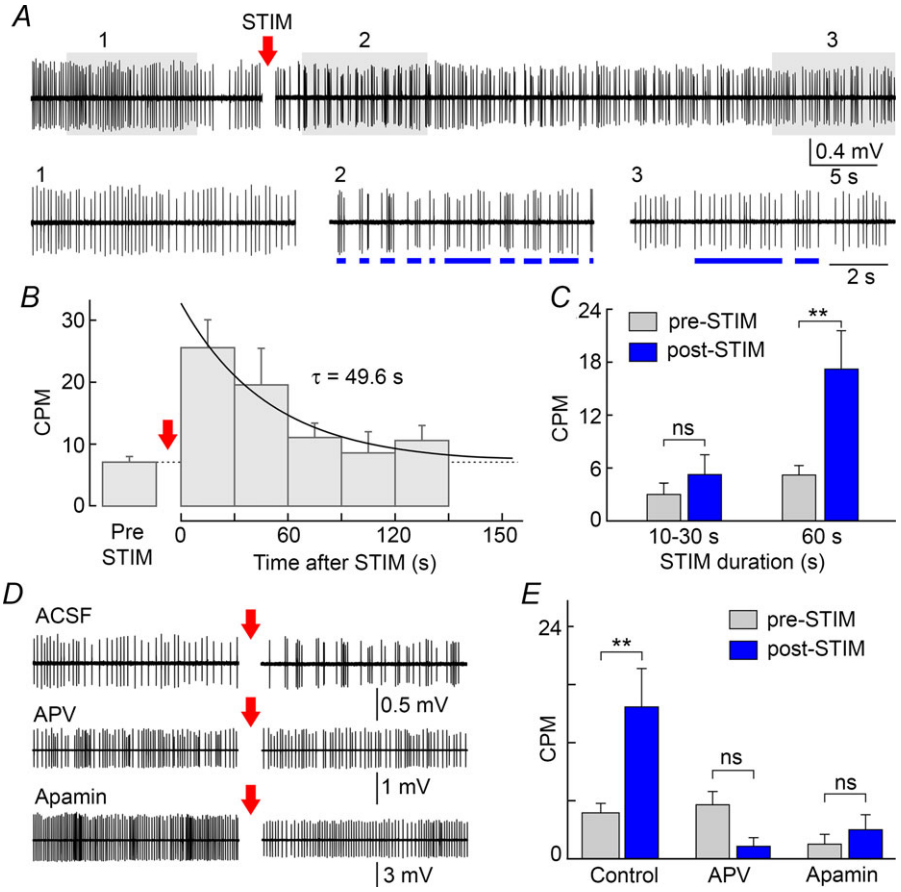

Figure 1. OVLT stimulation induces spike clustering in MNCs
A, single unit spiking activity recorded from a SON MNC in a hypothalamic explant shows the effect of OVLT stimulation at 10 Hz (STIM) for 60 s (segment removed). Lower traces are segments expanded from the shaded parts of the main trace. STIM caused a reversible increase in spike clusters (blue lines). *B*, graph shows mean (± SEM) rate of clustering (clusters per minute, CPM) before (pre-STIM; dashed line) and during 5 consecutive 30 s segments after STIM (post-STIM). Continuous line is a mono-exponential fit. *C*, bar graphs show mean (± SEM) CPM pre-STIM and during the first 20 s post-STIM observed when STIM was applied for 10–30 s or 60 s. *D*, spiking activity recorded from MNCs before and after STIM in control conditions (ACSF), or in the presence of APV or apamin. *E*, bar graphs show mean CPM observed pre- and post-STIM in different conditions. $^{**}P < 0.01$; ns, not significant.

−52.5 mV, and completely eliminated the presence of clustering activity at voltages ≥−50 mV (Fig. 3*D; n* = 12 for apamin and NMDA; paired *t* test). The duration of clusters recorded at equal levels of holding current was increased by 4 nM apamin (Fig. 3*E*). Moreover, 4 nM apamin decreased the mean maximal rate of clustering observed in the cells (Fig. 3*F*; from 10.6 ± 0.7 to 6.1 ± 1.3 CPM; $P = 0.0016$; $n = 12$) and this effect was accompanied by a significant increase in cluster duration (Fig. 3*F*; from 1.24 ± 0.14 to 4.76 ± 2.35 s; $n = 12$; paired *t* test; $P = 0.003$), but no change in mean intra-burst spiking frequency (Fig. 3*F*; paired *t* test; $P = 0.464$). Therefore partial inhibition of SK channel activity can effectively modulate NMDAR-induced clustering activity in MNCs.

Previous work showed that NT can both depolarize the membrane potential and reduce the after-hyperpolarization amplitude in MNCs (Kirkpatrick & Bourque, 1995). We therefore examined if NT could modulate NMDAR-dependent clustered firing. We first determined which G-protein coupled NT receptors (NTS) are expressed in the SON using tissue RT-PCR. As illustrated in Fig. 4*A*, transcripts encoding both NTS1 and NTS2 could be detected within the SON. However, single cell RT-PCR in acutely isolated SON neurons revealed that most MNCs express NTS2 rather than NTS1. As shown in Fig. 4*B–D*, application of 0.3–3 μM $NT^{8–13}$, a fragment that activates NTS2 (Vincent *et al.* 1999), significantly reduced clustering activity (from 9.8 ± 1.7 to 4.4 ± 1.2 CPM in $NT^{8–13}$; $n = 17$; paired *t* test;

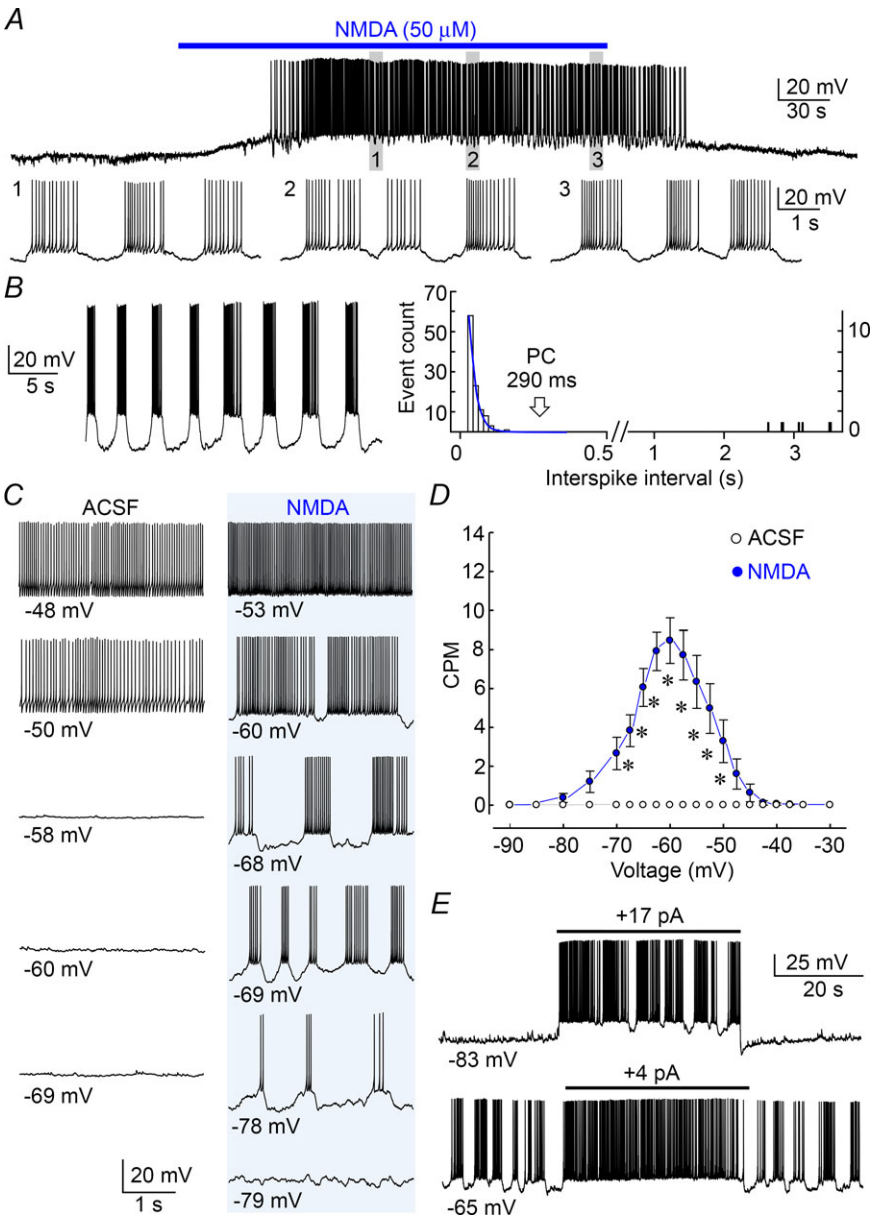

Figure 2. Voltage dependence of NMDAR-induced clustering
A, upper trace shows a whole-cell voltage recording from a MNC in a hypothalamic slice (excerpts shown below). Bath application of NMDA (bar) caused a reversible depolarization and sustained clustering activity. *B*, left trace shows an example of NMDA-induced clustering in another MNC. The histogram at right plots the distribution of interspike intervals for the corresponding cell. The blue curve is a single exponential fit of the falling phase of the distribution. The arrow points to the pause criterion (PC), beyond which intervals of greater duration are defined as pauses (see Methods). *C*, recording segments from a single MNC illustrate the relation between voltage (average of all points, indicated below) and firing pattern in absence (ACSF) or presence of NMDA. Each trace was recorded with different levels of holding current (not shown). *D*, graph shows mean (±SEM) clustering rate at different voltages in ACSF and NMDA (*$P < 0.05$). *E*, traces from MNCs exposed to NMDA show the effects of depolarizing current pulses (bars) applied from different baseline voltages.

$P = 0.0018$). However, bath application of 3 μM NT^{1-7}, an inactive fragment of NT (Kirkpatrick & Bourque, 1995), did not affect the rate of NMDA-induced clustering (from 12.3 ± 1.7 to 11.3 ± 2.2 CPM in NT^{1-7}; $n = 6$; paired t test; $P = 0.625$; Fig. 4*C* and *D*). Moreover, the effect of NT^{8-13} was prevented when tested in the presence of the NTS1/2 antagonist SR4692 (from 11.7 ± 1.5 to 10.1 ± 1.5 CPM; $n = 12$; paired t test; $P = 0.0711$; Fig. 4*C* and *D*). As illustrated in Fig. 4*E*, NT^{8-13} also significantly increased cluster duration (from 4.5 ± 1.0 to 22.9 ± 6.1 s in NT^{8-13}; $n = 17$; paired t test; $P = 0.002$) and this effect was also abolished by SR46892 (from 3.1 ± 0.4 to 3.2 ± 0.9 s; $n = 12$; paired t test; $P = 0.677$). NT^{1-7} had no effect on cluster duration (from 2.3 ± 0.4 to 2.9 ± 0.6 s; $n = 6$; paired t test; $P = 0.129$; Fig. 4*E*). To determine if the effects of NT^{8-13} on clustering were mediated by the peptide's depolarizing action, we also compared NMDA-induced clustering parameters on cells whose voltage was adjusted to −60 mV. As shown in Fig. 4*F*, NT^{8-13} had no significant effect on the rate of clustering observed at −60 mV ($n = 11$; paired t test; $P = 0.492$). However the increase in cluster duration ($n = 11$; paired t test; $P = 0.024$) and total number of action potentials recorded per 30 s test period ($P = 0.029$) were both significantly increased by NT^{8-13} in cells maintained at −60 mV. Lastly, we examined if NT can modulate NMDAR-dependent clustering induced by endogenous glutamate release in hypothalamic explants. As illustrated in Fig. 4*G* and *H*, bath application of NT^{8-13}

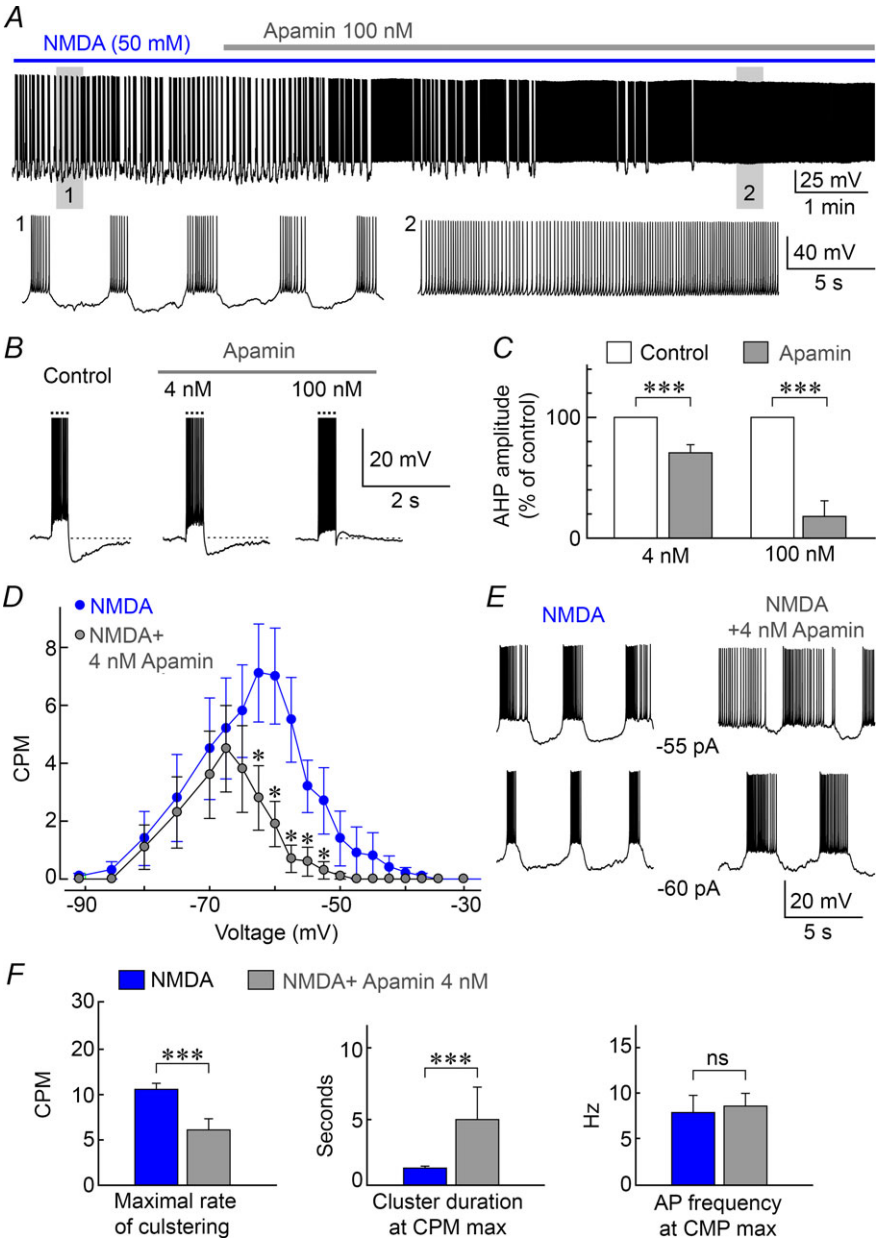

Figure 3. Inhibiting SK channels modulates spike clustering
A, voltage recording shows the effect of 100 nM apamin (grey bar) on NMDA-induced clustering (blue bar). Lower panels show excerpts of the full trace (as indicated by numbers). *B*, traces show the effects of apamin on after-hyperpolarizations (AHPs) induced by spike trains triggered by depolarizing current pulses (dotted lines). *C*, bar graphs show the effects of 4 nM and 100 nM apamin on mean (±SEM) AHP amplitude expressed as percentage of control. *D*, graph shows the effect of 4 nM apamin on mean (±SEM) clustering rate observed at different voltages. *E*, traces show the effects of apamin on NMDA-induced clustering activity at fixed levels of current injection (shown). *F*, bar graphs show the effects of 4 nM apamin on mean (±SEM) maximal clustering rate (CPM max), as well as cluster duration and intracluster spiking frequency at CPM max. $^{*}P < 0.05$; $^{***}P < 0.005$; ns, not significant.

abolished the increase in spike clustering induced by electrical stimulation (10 Hz, 60 s) of the OVLT ($n = 12$; one-way RM ANOVA with *post hoc* Holm–Sidak test; $P = 0.952$).

Discussion

The neurons recorded in our study were not specifically identified as vasopressin releasing MNCs. Previous studies have shown that the rat SON also contains oxytocin-releasing neurons, which account for approximately 35% of the total population of MNCs in this nucleus (Rhodes *et al.* 1979). It is therefore likely that both types of MNCs were sampled in our experiments. However, we found that all neurons recorded ($n = 70$) could display pronounced clustering activity upon exposure to NMDA, suggesting that both oxytocin- and vasopressin-releasing MNCs are capable of expressing NMDAR-dependent clustering activity. Interestingly, previous studies have shown that bursting activity

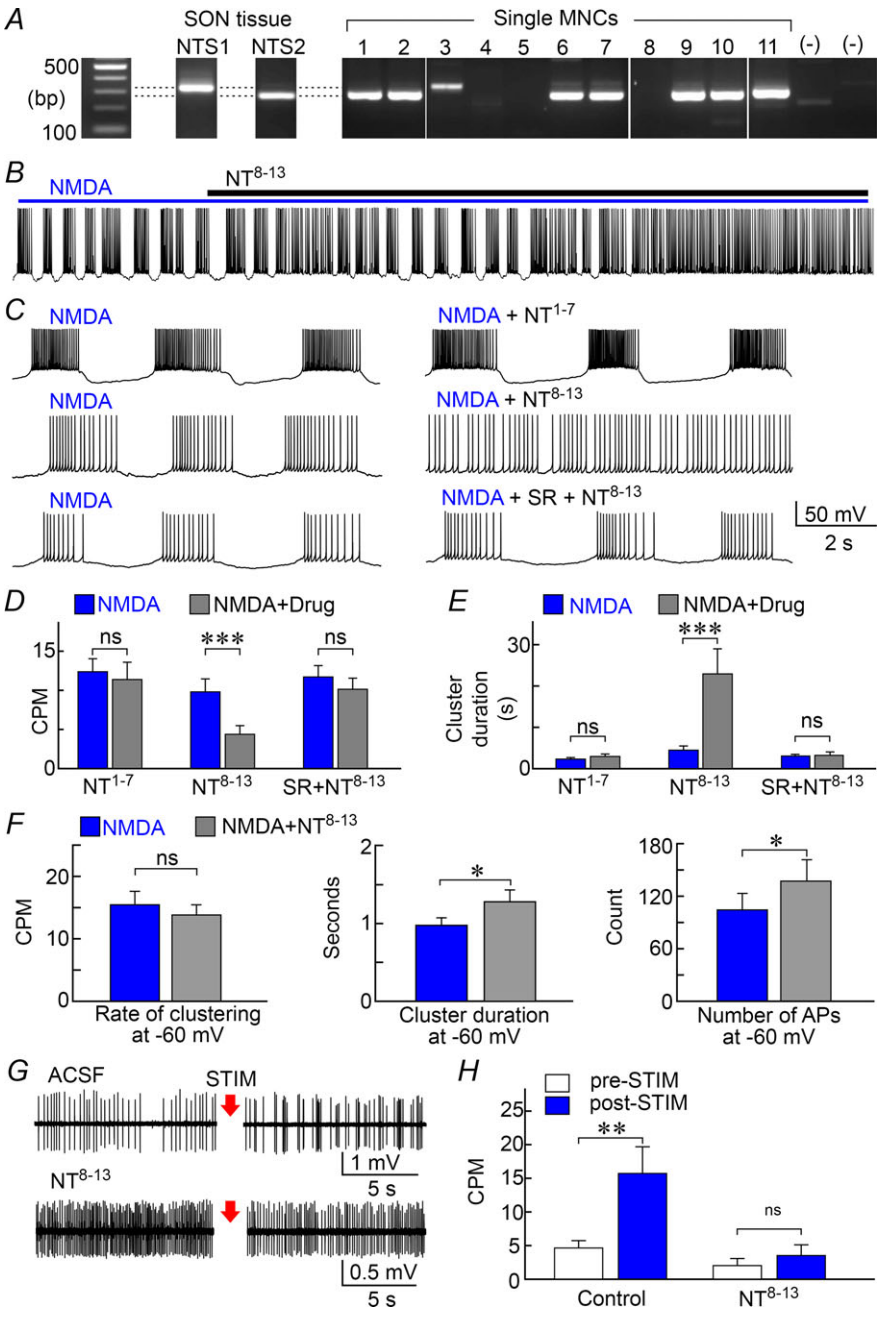

Figure 4. NT receptors modulate NMDAR-dependent clustering in MNCs
A, PCR detection of mRNAs coding for NTS1 and NTS2 in SON tissue, and in 11 single MNCs ((–) lanes are controls). *B*, whole-cell recording from an MNC exposed to NMDA shows that addition of $NT^{8–13}$ inhibits clustering. *C*, excerpts taken from 3 cells show NMDA-induced activity recorded before (left) and after (right) addition of $NT^{1–7}$, $NT^{8–13}$ or $NT^{8–13}$+SR46892 (SR). *D* and *E*, bar graphs show the mean (±SEM) rate of clustering (*D*) and cluster duration (*E*) observed in the presence of NMDA alone (blue) or in the presence of NMDA and various drugs (grey bars, drugs indicated below each set). *F*, bar graphs show mean (±SEM) values of clustering rate, cluster duration and total number of action potentials (count) in the absence (blue) and presence of $NT^{8–13}$ (grey) in cells whose voltage was adjusted to a value of −60 mV for both conditions. *G*, single unit recordings from MNCs in hypothalamic explants show the effects of stimulating the OVLT for 60 s at 10 Hz (STIM; arrows) in the absence (ACSF) and presence of $NT^{8–13}$. *H*, bar graphs show the effect $NT^{8–13}$ on mean (±SEM) rates of clustering induced by OVLT stimulation. $^*P < 0.05$; $^{**}P < 0.01$; $^{***}P < 0.005$; ns, not significant.

can also facilitate the release of oxytocin from the neurohypophysis (Bicknell, 1988). Although we believe that the results reported in our study are applicable to both oxytocin- and vasopressin-releasing MNCs, additional work is needed to establish if the modulation of clustering activity contributes to the regulation of both types of hormones *in vivo*.

A considerable amount of information has been accumulated concerning phasic activity in SON neurons (Wakerley *et al.* 1978) and effective computational models have been developed using quantitative electrophysiological data (Roper *et al.* 2004; MacGregor & Leng, 2012). However, little is known about clustered activity, a firing pattern that emerges during hyperosmolality (Bourque & Renaud, 1984; Poulain *et al.* 1988) and which enhances activity-dependent hormone release from the posterior pituitary (Cazalis *et al.* 1985). Our findings show that sustained electrical stimulation of the OVLT, which contains neurons that are excited by hyperosmolality and which release glutamate from axon terminals in the SON (Armstrong *et al.* 1996; Bourque, 2008), causes an enhancement of spike clustering in MNCs. This effect was prevalent at a stimulation frequency of 10 Hz, a value which corresponds to the firing rate of rat OVLT neurons exposed to a hypertonic stimulus (Vivas *et al.* 1990). Indeed, previous work has shown that stimulation of the OVLT can activate NMDARs (Yang *et al.* 1994; Panatier *et al.* 2006), and our current data indicate that OVLT-mediated clustering is inhibited by blocking NMDARs. Taken together, these observations indicate that endogenous glutamate release can induce clustering in MNCs through the activation of NMDARs.

OVLT-mediated clustering activity persisted for a significant amount of time following the end of a stimulation trial. Specifically, kinetic analysis revealed that the rate of clustering returned to baseline following an exponential time course with a time constant of ∼50 s. The basis for this persistence remains to be determined, but several mechanisms could be involved. First, MNCs express a high density of GLUN2D (Doherty & Sladek, 2011), an NMDAR subunit that features an unusually slow offset decay ($\tau \sim 5$ s; Monyer *et al.* 1994). Second, it has been shown that quantal glutamate release persists for tens of milliseconds following the arrival of a single action potential into presynaptic axon terminals contacting MNCs (Iremonger & Bains, 2007). Moreover, repetitive stimulation of afferents at 10 Hz has been shown to enhance glutamate release probability for ≥60 s after the end of a stimulus (Kombian *et al.* 2000). Third, it is possible that prolonged high frequency stimulation of the OVLT causes an accumulation of glutamate that exceeds the capacity of local transporters such that synaptic NMDARs remain activated for a protracted period following a train of stimuli. Fourth, it is also possible that repetitive activation of axon terminals causes a spill-over of glutamate into the extrasynaptic space, where it could lead to a prolonged activation of extrasynaptic NMDARs. Indeed, a recent study has shown that extrasynaptic NMDARs contribute to the excitation of MNCs during dehydration (Joe *et al.* 2014). Additional studies are required to define the mechanisms responsible for the persistent activation of clustering after OVLT stimulation in MNCs.

NMDAR-mediated rhythmic clustering activity has been shown to depend on apamin-sensitive (SK type) calcium-dependent K^+ channels (Hu & Bourque, 1992) which play an important role in controlling burst duration by promoting an activity-dependent after-hyperpolarization (Bourque & Brown, 1987). Indeed bath application of a saturating concentration of apamin completely suppressed NMDAR-induced clustering and caused the cells to fire tonically. Interestingly, a partial inhibition of SK channels (∼25%) with 4 nM apamin caused a significant decrease in the rate of spike clustering and an increase in cluster duration. These results show that even partial modulation of SK channels could provide an effective mechanism for the regulation, or fine tuning, of spike clustering in MNCs. Previous studies have shown that receptor-dependent modulation of SK channels can be achieved through membrane trafficking (Faber, 2009) or phosphorylation (Adelman *et al.* 2012).

Although we cannot exclude the possibility that presynaptic NMDARs contribute to NMDA-induced spike clustering, we found that NMDA can induce spike clustering in acutely isolated MNCs, which are devoid of presynaptic contacts (H. Hiruma and C. Bourque, unpublished results). Moreover the strong sensitivity of clustering to changes in postsynaptic voltage argues strongly that postsynaptic receptors are involved. Indeed we found that the rate of spike clustering varies as a bell-shaped function of membrane voltage with a peak near −60 mV. The sharp increase in clustering rate observed between −67.5 and −60 mV (Fig. 2*D*) presumably reflects the removal of Mg^{2+} block of the NMDARs over this range of voltages (Panatier *et al.* 2006). Indeed, current injection experiments showed that small depolarizing stimuli applied from voltages below −60 mV can promote clustering activity. On the other hand, the progressive increase in cluster duration and decrease in clustering rate observed between −60 and −50 mV is likely to be due to the fact that as the neurons become more depolarized the ability of SK channels to initiate pauses becomes attenuated, until a voltage is reached at which pauses can no longer be elicited and the cell fires tonically. Neurotransmitter-mediated changes in membrane voltage could therefore modulate the degree of clustered firing induced by glutamatergic afferents.

To determine if NMDAR-dependent spike clustering can be modulated by the activation of other receptors we

investigated the effect of the tridecapeptide NT, which has been reported to inhibit the SK channel-mediated after-hyperpolarization and to depolarize MNCs in the SON (Kirkpatrick & Bourque, 1995; Chakfe & Bourque, 2000). Although the SON was found to express both NTS1 and NTS2 receptors, single cell RT-PCR analysis showed that MNCs preferentially express the NTS2 receptor. Bath application of $NT^{8–13}$, which activates NTS2 (Vincent *et al.* 1999) significantly increased cluster duration and reduced the overall rate of spike clustering in MNCs. These effects were abolished by SR 48692, an antagonist of both NTS1 and NTS2 receptors (Pelaprat, 2006) and could not be induced by the inactive agonist $NT^{1–7}$.

Interestingly the effects of $NT^{8–13}$ on the rate of clustering were eliminated when cell voltage was restored to control value (Fig. 4*F*), suggesting that this effect depends mainly on the peptide's depolarizing effect. However, $NT^{8–13}$ significantly prolonged cluster duration and increased the total number of action potentials recorded per test segment, even when voltage was maintained at an equivalent level in the absence and presence of the peptide (Fig. 4*F*). Thus the effects of $NT^{8–13}$ on these parameters may involve additional actions, such as the regulation of SK channels, or other conductances. The mechanisms by which $NT^{8–13}$ modulate these parameters remains to be determined.

Taken together, these findings demonstrate that endogenous glutamate release can induce spike clustering in MNCs, via activation of NMDARs and SK channels. Moreover, we show that modulation of SK channels, or the resting potential of MNCs, provides an effective mechanism for the fine tuning of clustering activity. Indeed, many neuromodulators, including NT, have been shown to provoke slow changes in membrane potential in MNCs (Renaud & Bourque, 1991; Chakfe & Bourque, 2000). Whether such mechanisms are involved in regulating the expression of clustering during dehydration or hypertonicity remains to be determined.

References

Adelman JP, Maylie J & Sah P (2012). Small-conductance Ca^{2+}-activated K^+ channels: form and function. *Annu Rev Physiol* **74**, 245–269.

Armstrong WE, Tian M & Wong H (1996). Electron microscopic analysis of synaptic inputs from the median preoptic nucleus and adjacent regions to the supraoptic nucleus in the rat. *J Comp Neurol* **373**, 228–239.

Bicknell RJ (1988). Optimizing Release from peptide hormone secretory nerve terminals. *J Exp Biol* **139**, 51–65.

Bourque CW (2008). Central mechanisms of osmosensation and systemic osmoregulation. *Nat Rev Neurosci* **9**, 519–531.

Bourque CW & Brown DA (1987). Apamin and *d*-tubocurarine block the afterhyperpolarization of rat supraoptic neurosecretory neurons. *Neurosci Lett* **82**, 185–190.

Bourque CW & Renaud LP (1984). Activity patterns and osmosensitivity of rat supraoptic neurones in perfused hypothalamic explants. *J Physiol* **349**, 631–642.

Brown CH & Bourque CW (2006). Mechanisms of rhythmogenesis: insights from hypothalamic vasopressin neurons. *Trends Neurosci* **29**, 108–115.

Cazalis M, Dayanithi G & Nordmann JJ (1985). The role of patterned burst and interburst interval on the excitation-coupling mechanism in the isolated rat neural lobe. *J Physiol* **369**, 45–60.

Chakfe Y & Bourque CW (2000). Excitatory peptides and osmotic pressure modulate mechanosensitive cation channels in concert. *Nat Neurosci* **3**, 572–579.

Choe KY, Olson JE & Bourque CW (2012). Taurine release by astrocytes modulates osmosensitive glycine receptor tone and excitability in the adult supraoptic nucleus. *J Neurosci* **32**, 12518–12527.

Ciura S & Bourque CW (2006). Transient receptor potential vanilloid 1 is required for intrinsic osmoreception in organum vasculosum lamina terminalis neurons and for normal thirst responses to systemic hyperosmolality. *J Neurosci* **26**, 9069–9075.

Ciura S, Liedtke W & Bourque CW (2011). Hypertonicity-sensing in organum vasculosum lamina terminalis neurons: a mechanical process involving Trpv1 but not Trpv4. *J Neurosci* **31**, 14669–14676.

Doherty FC & Sladek CD (2011). NMDA receptor subunit expression in the supraoptic nucleus of adult rats: dominance of NR2B and NR2D. *Brain Res* **1388**, 89–99.

Dutton A & Dyball RE (1979). Phasic firing enhances vasopressin release from the rat neurohypophysis. *J Physiol* **290**, 433–440.

Faber ES (2009). Functions and modulation of neuronal SK channels. *Cell Biochem Biophys* **55**, 127–139.

Hu B & Bourque CW (1992). NMDA receptor-mediated rhythmic bursting activity in rat supraoptic nucleus neurones *in vitro*. *J Physiol* **458**, 667–687.

Iremonger KJ & Bains JS (2007). Integration of asynchronously released quanta prolongs the postsynaptic spike window. *J Neurosci* **27**, 6684–6691.

Joe N, Scott V & Brown CH (2014). Glial regulation of extrasynaptic NMDA receptor-mediated excitation of supraoptic nucleus neurones during dehydration. *J Neuroendocrinol* **26**, 35–42.

Kirkpatrick K & Bourque CW (1995). Effects of neurotensin on rat supraoptic nucleus neurones *in vitro*. *J Physiol* **482**, 373–381.

Ko D, Wilson CJ, Lobb CJ & Paladini CA (2012). Detection of bursts and pauses in spike trains. *J Neurosci Methods* **211**, 145–158.

Kombian SB, Hirasawa M, Mouginot D, Chen X & Pittman QJ (2000). Short-term potentiation of miniature excitatory synaptic currents causes excitation of supraoptic neurons. *J Neurophysiol* **83**, 2542–2553.

Krahe R & Gabbiani F (2004). Burst firing in sensory systems. *Nat Rev Neurosci* **5**, 13–23.

McGinty D & Szymusiak R (1988). Neuronal unit activity patterns in behaving animals: brainstem and limbic system. *Ann Rev Psych* **39**, 135–168.

MacGregor DJ & Leng G (2012). Phasic firing in vasopressin cells: understanding its functional significance through computational models. *PLoS Comput Biol* **8**, e1002740.

Monyer H, Burnashev N, Laurie DJ, Sakmann B & Seeburg PH (1994). Developmental and regional expression in the rat brain and functional properties of four NMDA receptors. *Neuron* **12**, 529–540.

Panatier A, Gentles SJ, Bourque CW & Oliet SH (2006). Activity-dependent synaptic plasticity in the supraoptic nucleus of the rat hypothalamus. *J Physiol* **573**, 711–721.

Pelaprat D (2006). Interactions between neurotensin receptors and G proteins. *Peptides* **27**, 2476–2487.

Poulain DA, Brown D & Wakerley JB (1988). Statistical analysis of patterns of electrical activity in vasopressin- and oxytocin-secreting neurons. In *Pulsatily in Neuroendocrine Systems*, ed. Leng G, pp. 119–154. CRC Press, Boca Raton, FL, USA.

Renaud LP & Bourque CW (1991). Neurophysiology and neuropharmacology of hypothalamic magnocellular neurons secreting vasopressin and oxytocin. *Prog Neurobiol* **36**, 131–169.

Rhodes CH, Morrell JI & Pfaff DW (1981). Immunohistochemical analysis of magnocellular elements in rat hypothalamus: distribution and numbers of cells containing neurophysin, oxytocin, and vasopressin. *J Comp Neurol* **198**, 45–64.

Richard D & Bourque CW (1995). Synaptic control of rat supraoptic neurones during osmotic stimulation of the organum vasculosum lamina terminalis *in vitro*. *J Physiol* **489**, 567–577.

Roper P, Callaway J & Armstrong W (2004). Burst initiation and termination in phasic vasopressin cells of the rat supraoptic nucleus: a combined mathematical, electrical, and calcium fluorescence study. *J Neurosci* **24**, 4818–4831.

Sharif Naeini R, Witty MF, Seguela P & Bourque CW (2006). An N-terminal variant of Trpv1 channel is required for osmosensory transduction. *Nat Neurosci* **9**, 93–98.

Trudel E & Bourque CW (2010). Central clock excites vasopressin neurons by waking osmosensory afferents during late sleep. *Nat Neurosci* **13**, 467–474.

Vincent JP, Mazella J & Kitabgi P (1999). Neurotensin and neurotensin receptors. *Trends Pharmacol Sci* **20**, 302–309.

Vivas L, Chiaraviglio E & Carrer HF (1990). Rat organum vasculosum laminae terminalis *in vitro*: responses to changes in sodium concentration. *Brain Res* **519**, 294–300.

Wakerley JB, Poulain DA & Brown D (1978). Comparison of firing patterns in oxytocin- and vasopressin-releasing neurones during progressive dehydration. *Brain Res* **148**, 425–440.

Yang CR, Senatorov VV & Renaud LP (1994). Organum vasculosum lamina terminalis-evoked postsynaptic responses in rat supraoptic neurones *in vitro*. *J Physiol* **477**, 59–74.

Additional information

Competing interests

The authors have no conflicts of interest to declare regarding the data and information provided in this manuscript.

Author contributions

Conception and design of the experiments: A.G., C.W.B.; collection, analysis and interpretation of data: A.G., M.W., T.O., C.Z., K.Y.C.; drafting the article or revising it critically for important intellectual content: A.G., C.W.B. All authors have approved the final version of the manuscript. All persons designated as authors qualify for authorship, and all those who qualify for authorship are listed.

Funding

This work was supported by Canadian Institutes of Health Research (CIHR) Operating grant MOP-9939 to C.W.B, who was also recipient of a James McGill Research Chair. The Research Institute of the McGill University Health Center is supported by the Fonds de Recherche du Québec-Santé (FRQS).

Acknowledgements

The authors thank Dr Philippe Sarret (Université de Sherbrooke, QC) for kindly providing SR46892.